Electronic Supplementary Material (ESI) for Chemical Communications.

Gd-based MRI contrast agents for Zn detection: the role of local accumulation in vivo

Kyangwi P. Malikidogo, Manon Isaac, Adrien Uguen, Sandra Même, Agnès Pallier, Rudy Clémençon, Jean-François Morfin, Sara Lacerda, Eva Toth, Célia S. Bonnet

Experimental Section

General remarks

$ZnCl_2$, $GdCl_3$, HEPES and fatty acid free albumin from human serum were purchased from Sigma Aldrich.

Liquid sample preparation

The ligand concentrations were determined by adding an excess of zinc solution to a ligand solution and titrating the metal excess with standardized Na_2H_2EDTA in urotropine buffer (pH 5.6–5.8) in the presence of Xylenol Orange as an indicator. The concentration of the metal solutions was determined similarly by complexometric titrations. The complexes were prepared by mixing 1 eq. of L, with 1 eq. of Gd^{3+}, and the pH was adjusted to 7.4 either with a buffered solution or by adding KOH or HCl to the solution. The absence of free Gd^{3+} was checked by the Xylenol orange test. The concentrations of Gd^{3+}-containing solutions were also checked both by ICP-OES and BMS.

Dissociation kinetic studies

The kinetic inertness of Gd**PyC4mDPA** and GdPy were assessed at 25 °C and in 0.1 M NaCl, via transmetallation studies of GdL (100 µM) with Eu^{3+} (10-fold excess) at pH 3.55; 3.64; 3.68; 3.81; 3.99; 4.11 and 4.55 (0.02 M dimethyl-piperazine), and pH 5.03 (0.02 M N-methylpiperazine). Similar experiments were performed with 20, 30 and 40-fold excess of Eu^{3+} at pH 3.81, and 40-fold excess of Eu^{3+} at pH 4.6 and 3.95. The excess of the exchanging metal ion guarantees the pseudo-first order conditions. The pH was controlled for each sample at the end of the kinetic measurements to confirm

that it remained stable during the experiment. In all cases, the reactions were monitored by measuring the Eu^{3+} emission on an Agilent Cary Eclipse Fluorescence spectrophotometer. The analysis of the experimental data was performed using Visualiseur/Optimiseur running on a MATLAB 8.3.0 (R2014a) platform.[1]

In the presence of high excess of Eu^{3+} (10-40 folds), to ensure pseudo first order conditions, the dissociation of **GdPyC4mDPAH** is expressed in Equation (1).

$GdLH + Eu^{3+} = EuLH + Gd^{3+}$ (1)

In such conditions, the reaction rate can be expressed by eq. 2, where k_{obs} is a pseudo-first-order rate constant and $[GdLH]_t$ is the total complex concentration:

$$-\frac{d[GdLH]_t}{dt} = k_{obs}[GdLH]_t \quad (2)$$

No significant variations on the k_{obs} values were observed depending on the Eu^{3+} concentration, which does not evidence any metal assisted dissociation.

The overall dissociation mechanism is illustrated in Scheme 1.

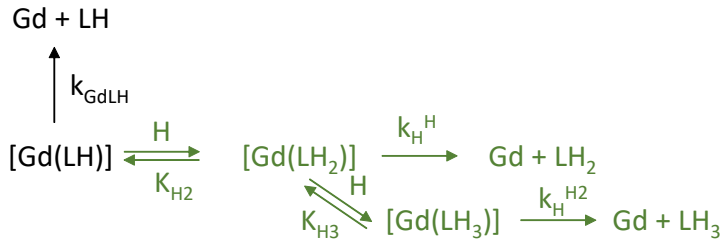

Scheme 1: Reaction mechanism of the dissociation of GdLH (charges are omitted for clarity)

The concentration of **GdPyC4mDPAH** can be given as the sum of the concentrations of the different reactive species (eq. 3):

$[GdLH]_t = [Gd(LH)] + [Gd(LH_2)] + [Gd(LH_3)]$ (3)

Considering the relevant complex protonation constants ($K_2 = [GdLH_2]/[GdLH][H^+]$ and $K_3 = [GdLH_3]/[GdLH_2][H^+]$), the pseudo first-order rate constant k_{obs} can be expressed as follows :

$$k_{obs} = \frac{k_0 + k_1[H^+] + k_2[H^+]^2}{1 + K_H^H[H^+] + K_H^H K_H^{H2}[H^+]^2} \quad (4)$$

where $k_0 = k_{GdLH}$, $k_1 = k_H^H K_2$, $k_2 = k_H^{H2} K_2 K_3$

Equation (4) could be simplified to equation (5) in the final treatment :

$$k_{obs} = k_1[H^+] + k_2[H^+]^2 \quad (5)$$

Luminescent measurements

Fluorescence spectra were recorded on an Agilent Cary Eclipse Fluorescence spectrophotometer with the following settings: excitation at 260 nm and emission scanning between 400 and 700 nm with an emission filter 360-1100nm, slit widths 5 nm for excitation and emission wavelengths, at 37 °C. The mixtures in a 500 µL quartz cuvette with a 2x10 mm path length were incubated for 3 min before the measurements were taken. To determine the affinity of dansylated aminoacids for HSA, various amounts of dansylaminoacid were added to a solution of [HSA] = 5 µM in 10 mM HEPES buffer, pH 7.2. For the displacement experiments, various amount of the different compounds were added to a solution of [HSA] = 5 µM and [dansylglycine] = 10 µM in 10 mM HEPES buffer pH 7.2. All spectra were normalized, then imported in HypSpec 2014 (Hyperquad suite). All titrations were fitted taking into account two equilibria: HSA + DslAA = HSA-DslAA and HSA + GdL = HSA-GdL ($Kd_{HSA-GdL}$). The formation constant of HSA-dansylglycine was set at $\beta_{HSA-DslGly}$ = 5.47 and for HSA-dansylarginine at $\beta_{HSA-DslArg}$ =3.9, and the emission spectra of the dansylglycine in 10 mM HEPES buffer pH 7.2 was recorded and set in HypSpec.

Europium luminescence lifetimes were recorded using the decay of the emission intensity at 616 nm, following an excitation at 263 nm. Measurements were performed in H_2O and D_2O solutions at 0.47 mM in HEPES buffers 0.1 M at pH/pD 7, 25 °C. The settings were as follow: gate time: 0.05 ms; delay time: 0.1 ms; flash count: 1; Total decay time: 6 ms; 100 cycle. At least three decay curves were collected for each sample, all lifetimes were analyzed as monoexponential decays. The reported lifetimes are an average of at least three measurements. The number of water molecules directly coordinated to Eu^{3+} were obtained using the empirical equation developed by Horrocks et al.,[2] and Parker et al.[3]

Relaxometric measurements

Proton NMRD profiles were recorded on a Stelar SMARTracer Fast Field Cycling relaxometer (0.01-10 MHz) and a Bruker WP80 NMR electromagnet adapted to variable field measurements (20-80 MHz) and controlled by a SMARTracer PC-NMR console. The temperature was monitored by a VTC91 temperature control unit and maintained by a gas

flow. The temperature was determined by previous calibration with a Pt resistance temperature probe. The longitudinal relaxation rates ($1/T_1$) were determined in aqueous solutions.

Paramagnetic Relaxation Enhancement measurements were performed at 20 MHz and 37 °C with 0.3 mM of GdPyC4mDPA and variable concentration of HSA.
Maximal values for the dissociation constants (K_D) with HSA can be obtained by fitting Paramagnetic Relaxation Enhancement data (Figure S6) to equation (6).

$$R_{1p} = 10^3 \times [(r_1^f.c_1) + \frac{1}{2}(r_1^b - r_1^f) \times (c_{HSA} + c_1 + K_D - \sqrt{(c_{HSA} + c_1 + K_D)^2 - 4c_{HSA}.c_1})] \quad (6)$$

Where r_1^f and r_1^b are the proton relaxivities of the free and bound state, c_{HSA} and c_1 are the concentration of HSA and the complex, respectively.

Phantom MR images at 9.4 T

Phantoms of Gd**PyC4mDPA**, Gd**PyC4mDPA**Zn (0.2 mM in mouse serum) and mouse serum have been imaged together at 37 °C with a classical Bruker birdcage coil, 35 mm inner diameter, on a BioSpec 9.4 T spectrometer (Bruker, Wissembourg, France). A spin echo sequence was used, to acquire images of each sample with a fixed TE of 16 ms and a variable TR ranging from 100 ms to 3000 ms. Using IsaTool program, provided with Paravision 5.1, the T_1 relaxation time of each phantom was calculated, using an exponential fitting, from signal mean intensity over 1 cm^2 region of interest measured on the images of each phantom as function of TR. Gd**PyC4mDPA**, Gd**PyC4mDPA**Zn and serum have T_1 values of 552 ms, 567 ms, and 3500 ms, respectively.

Inductively Coupled Plasma Optical Emission Spectroscopy (ICP-OES)

ICP-OES measurements were performed with a a Jobin Yvon ULTIMA2 Spectrometer (Longjumeau, France) or an Agilent 5800 VDV. Standard Gd and Zn solutions were prepared from commercial solutions for ICP (Sigma-Aldrich, France) in 5% HNO_3 matrix. The samples were digested in conc HNO_3 for 48 h at room temperature followed by 18 h at 80 °C. The resulting solutions were then diluted 1:13.4, to reach 5% in HNO_3. Measurements were performed in triplicate, using the most accurate band

for Gd (342.246 nm) or Zn (213.857). Data are presented as mean±SEM (n = 3 for Gd and n = 6 for Zn).

In vivo studies

9-weeks-old swiss nude females were purchased from Charles River Laboratories (Saint Germain Nuelles, France). All animal experiments were carried out in accordance with the guidelines for animal experiments and under permission number 21933, from the French "Ministère de l'Enseignement Supérieur, de la Recherche et de l'Innovation". Magnetic resonance acquisitions were performed on a 9.4 T Biospec 94/20 superconducting magnet (Bruker, Wissembourg, France) with a shielded gradient set (950 mT m^{-1} maximum gradient amplitude) and a transmit-receive quadrature coil with an inner diameter of 38 mm. Animals were anesthetized by inhalation of 2% isoflurane then maintained during MR experiments at 1.5% (0.5 L min^{-1} mixed in air and oxygen with 1:1 ratio). The physiological body temperature was maintained inside the magnet by circulating warm water. A pressure sensor was used to monitor the respiration. Images were acquired first using a gradient echo (Ig-Flash) sequence to localize the mouse and the pancreas in the magnet with the following parameters: TE/TR = 4 ms/280 ms, flip angle = 20°, FOV size = 6x3 cm, matrix size = 256*256, slice thickness = 1 mm, to display 234×137 μm^2 in plane resolution for a duration of 6 min (10 accumulations). Then both T_1-weighted images (TE/TR = 16/500 ms) and T_2-weighted images (TE/TR = 100/2000 ms) were acquired to localize the pancreas with the following parameters (Rare sequence: FOV size = 6x3 cm, matrix size = 256*256, slice thickness = 1 mm). The Dynamic Contrast Enhancement (DCE) experiment consisted of a T_1-weighted RARE spin echo sequence (Rare factor=4, field of view = 6*6 cm, matrix =128*128, TR/TE = 16/500 ms, slice thickness = 500 µm). Two sagittal T_1-weighted images were acquired to cover different organs every 2 minutes during one hour. A solution of 20% of glucose was injected intraperitoneally (40 µL) via a catheter. The contrast agent was manually injected (44 µmol/kg; n = 3 for GdPyC4mDPA and GdPy and n = 5 for Vasovist®) 10 min after the beginning of the acquisition via a catheter placed in the caudal vein. Grey level means in the kidney, pancreas, spleen and liver were plotted as a function of time during one hour. After the MRI scans, mice were sacrificed, the organs of interest harvested (kidneys, liver, spleen, pancreas, bone, blood) and their Gd and Zn content determined by ICP-OES (see detailed ICP-OES protocol above). For comparison purposes, Gd-based biodistribution of control mice (n = 3 for GdPyC4mDPA and GdPy and n = 5 for Vasovist®) without glucose injection was also performed.

For ICP-OES experiments at 10 min, a similar protocol to that of the MRI experiments was used with an intraperitoneal injection of a solution of 20% of glucose (40 µl). After 10 min, the contrast agent was manually injected in the caudal vein and the mice were sacrificed 10 min after injection and the organs of interested were harvested (n = 3).

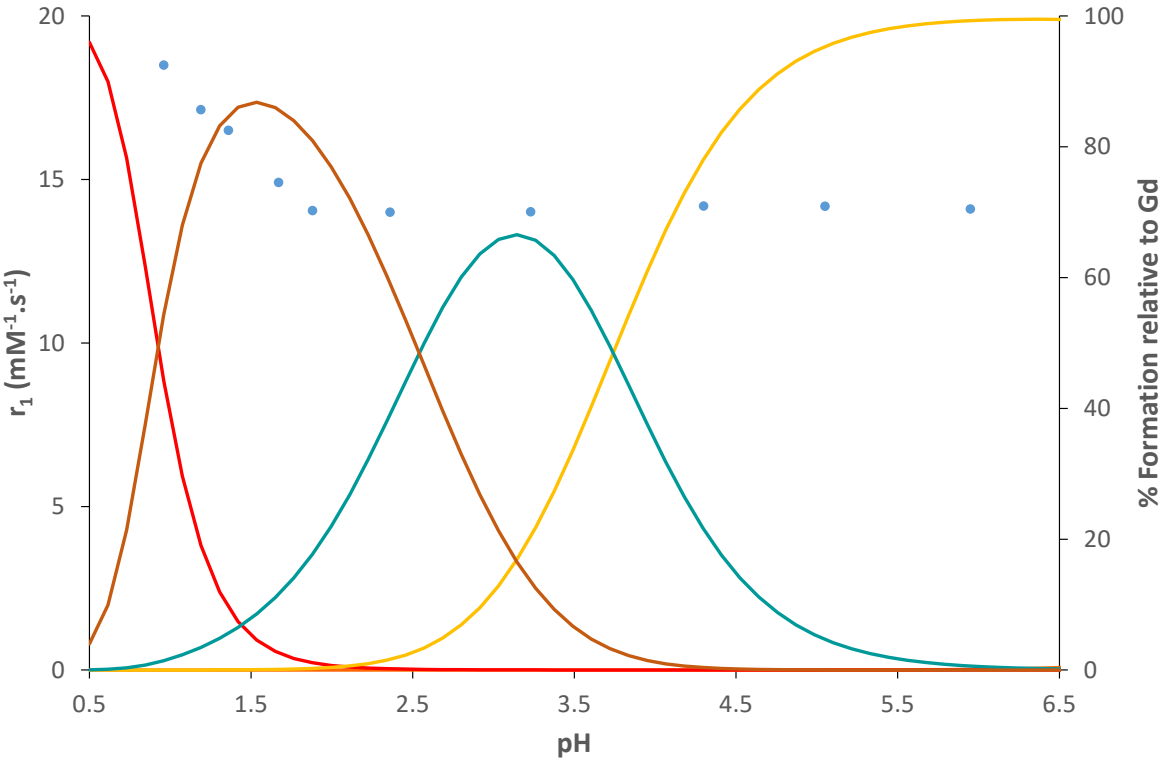

Figure S1: ^{1}H relaxivity measurements of an aqueous solution of [PyC4mDPA] = [Gd] = 0.373 mM (HEPES 0.1 M) as a function of pH, at 10 MHz and 298 K together with the species distribution calculated in the same conditions (free Gd; $GdLH_3$; $GdLH_2$; GdLH).

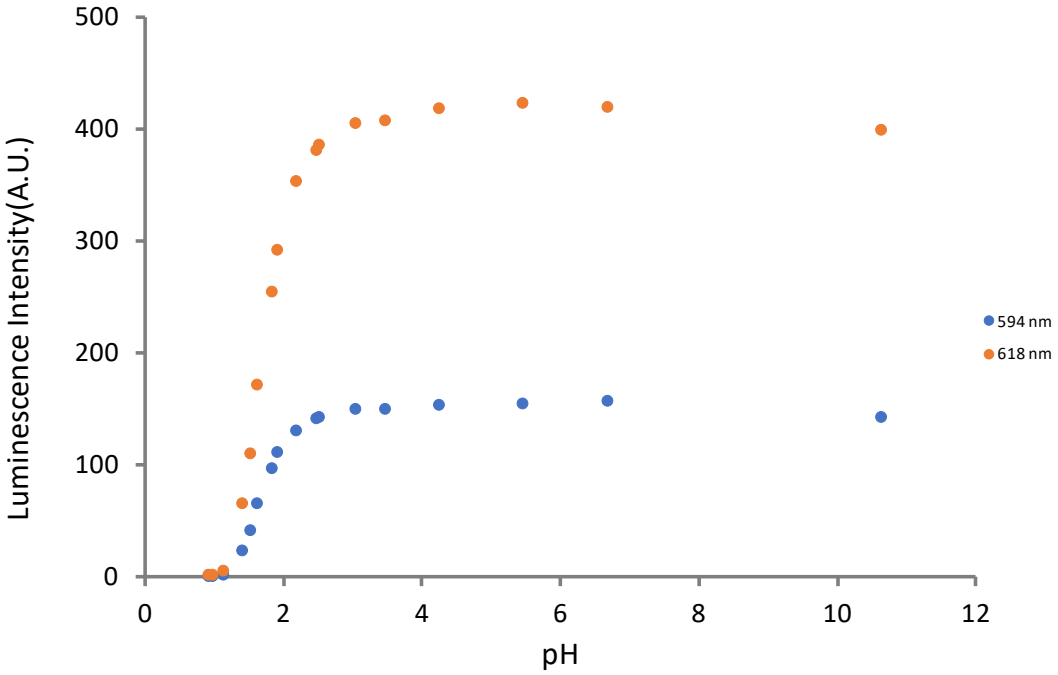

Figure S2: Luminescence titration of [PyC4mDPA] = 175.36 μM in the presence of 0.9 eq Eu^{3+} as a function of pH at λ_{em} = 594 nm and 618 nm.

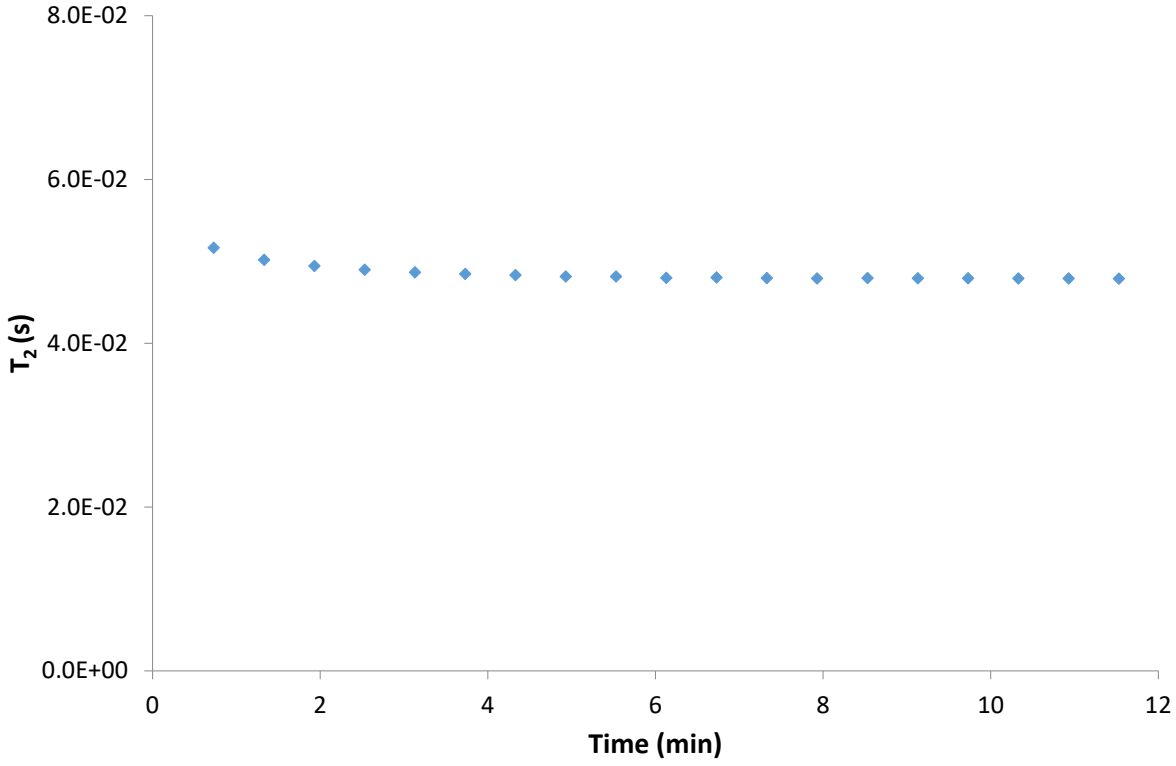

Figure S3: T_2 measurements of a solution of GdPy (0.5 mM) at pH 3.5 in the presence of 40 eq. of Cu^{2+}

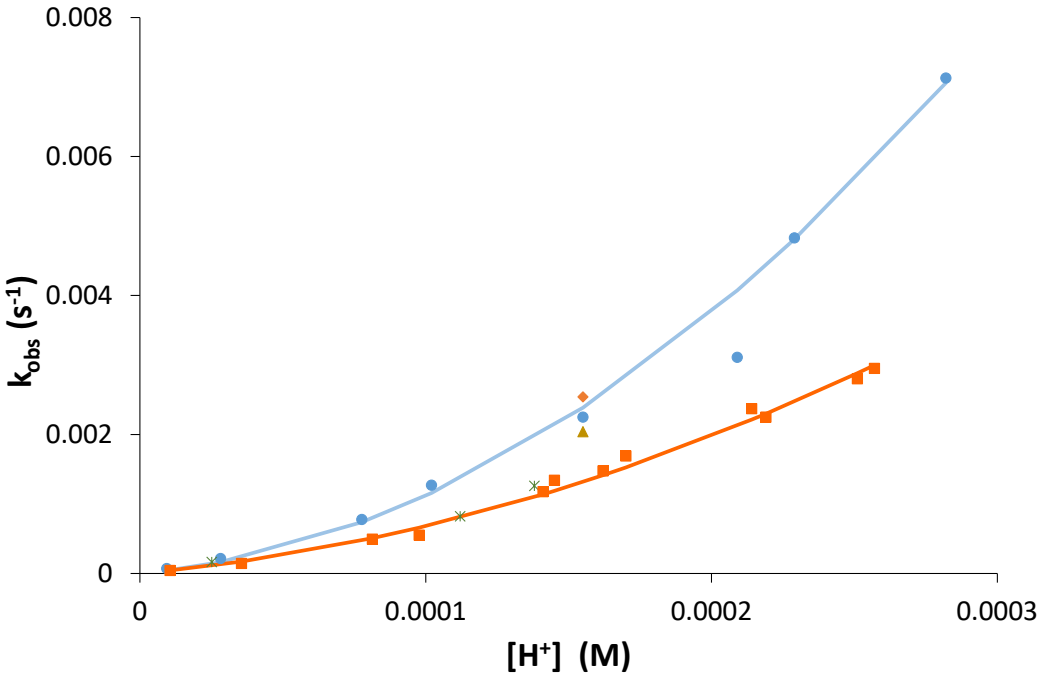

Figure S4: Observed dissociation rate constants, k_{obs}, as a function of proton concentration for the dissociation of GdPyC4mDPA (100 µM; ●) and GdPy (145 µM, ■) in the presence of 10 eq. of Eu^{3+}; GdPyC4mDPA (100 µM) with 20 eq. (◆), or 30 eq. (□), or 40 eq. (*) of Eu^{3+} at 25 °C in the presence of 0.1 M NaCl.

Table S1: Kinetic parameters and half-lives calculated from k_{obs} at pH 7.4 (25 °C, NaCl 0.1 M).

	GdPyC4mDPA	**GdPy**	**GdDTPA[a]**
$\mathbf{k_1}$ ($mol^{-1}.L.s^{-1}$)	3.6 (2)	3.7 (2)	0.58
$\mathbf{k_2}$ ($mol^{-2}.L^2.s^{-1}$)	7.60 (9).10^4	3.10 (8).10^4	9.7.10^4
$\mathbf{k_3^{Cu}}$ ($mol^{-1}.L.s^{-1}$)			0.93
$\mathbf{K_{GdLM}}$			13
$\mathbf{t_{1/2}}$ (pH 7/ h)	1342	1307	202

a. From Ref [4]; in 1 M KCl

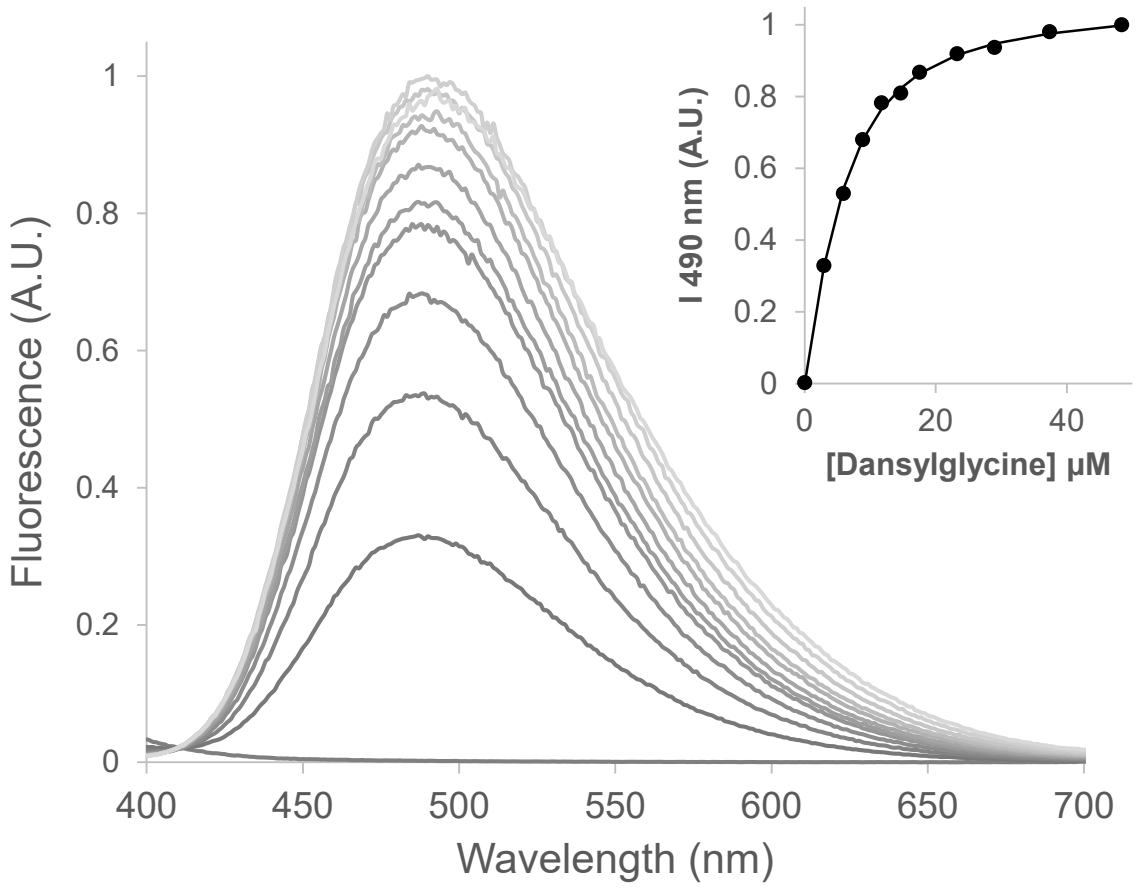

Figure S5: Fluorescence emission spectra of a solution of [HSA] = 5 µM (HEPES 0.1 M, pH = 7.4) upon Dansylglycine additions after excitation at 260 nm. Inset: Emission intensity at 490 nm (●) and the calculated intensities using HypSpec.

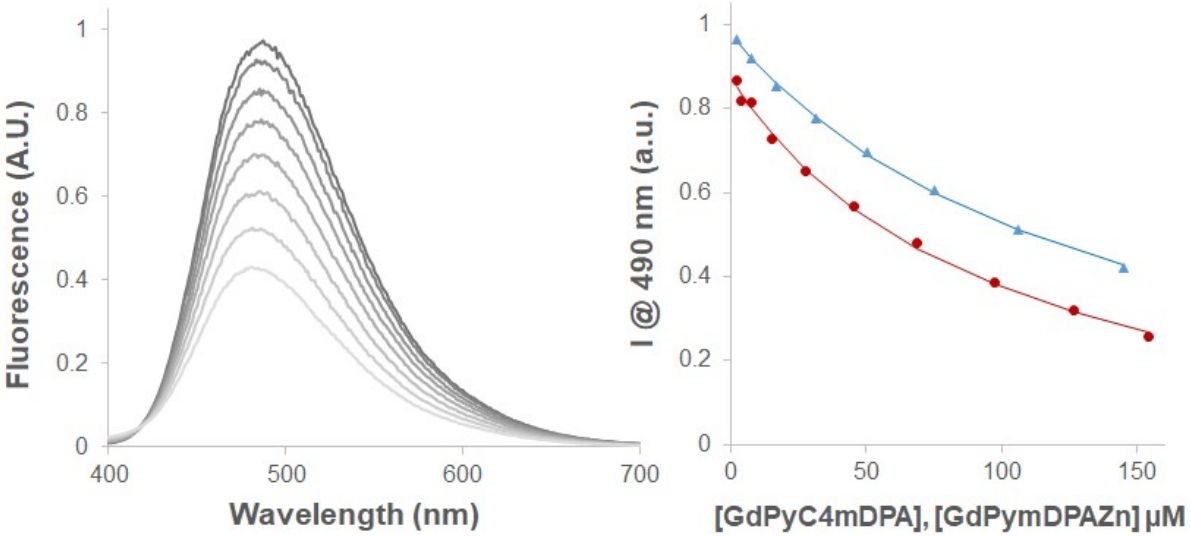

Figure S6: A) Fluorescence emission spectra of a solution of [HSA] = 5 µM (HEPES 0.1 M, pH = 7.4) and [Dansylglycine] = 10µM upon addition of **Gd PyC4mDPA** after

excitation at 260 nm. B) Emission intensity at 490 nm upon addition of **Gd PyC4mDPA** (①) or **GdPyC4mDPA** with 1 equivalent of Zn^{2+} (●). The lines represent the calculated intensities using HypSpec with the values presented Table 4.

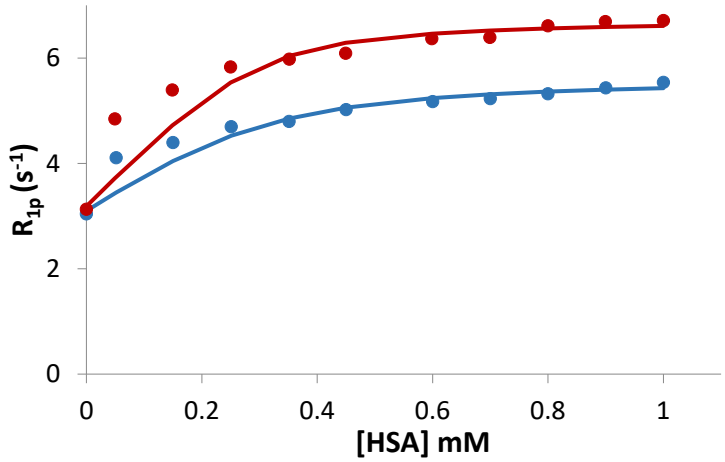

Figure S7: ^{1}H PRE measurements at pH = 7.4 (HEPES 0.1 M), 20 MHz, 310 K as a function of HSA concentration in the presence of [**GdPyC4mDPA**] = 0.3 mM, in the absence (blue) or in the presence of 1 eq. of Zn^{2+} (red) (E titration). The solid curves represent the fit to eq. 6 with the parameters from Table 1 in excess of HSA compared to **GdPyC4mDPA** to access the site of highest affinity.

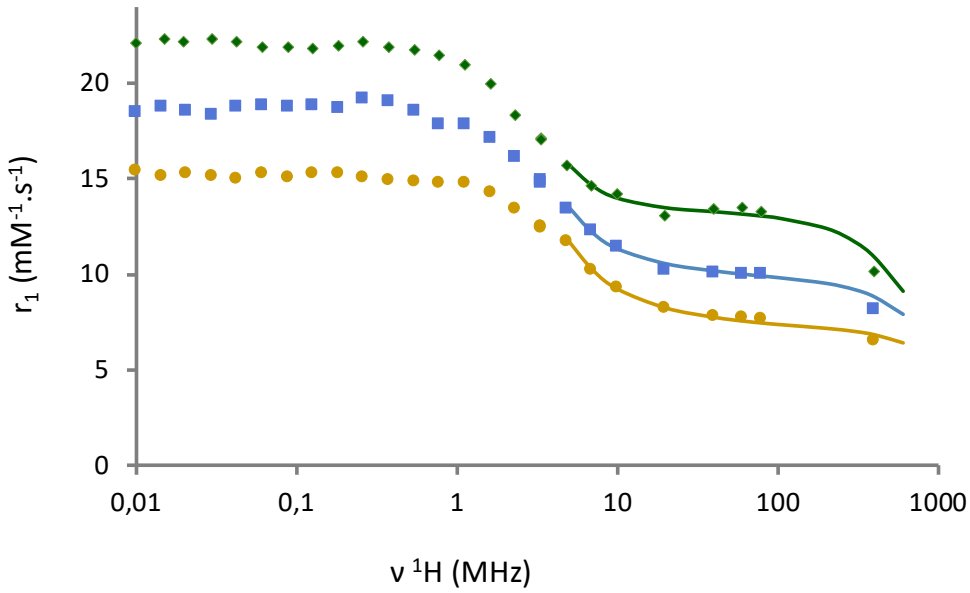

Figure S8: ^{1}H NMRD profiles of aqueous solutions containing [**GdPyC4mDPA**] = 1.01 mM (HEPES 0.1 M, pH = 7.4) at 298 K (♦), 310 K (■), and 323 K (●). The lines represent the least-squares fit of the data points using the Solomon-Bloembergen-Morgan theory using parameters from Table S4.

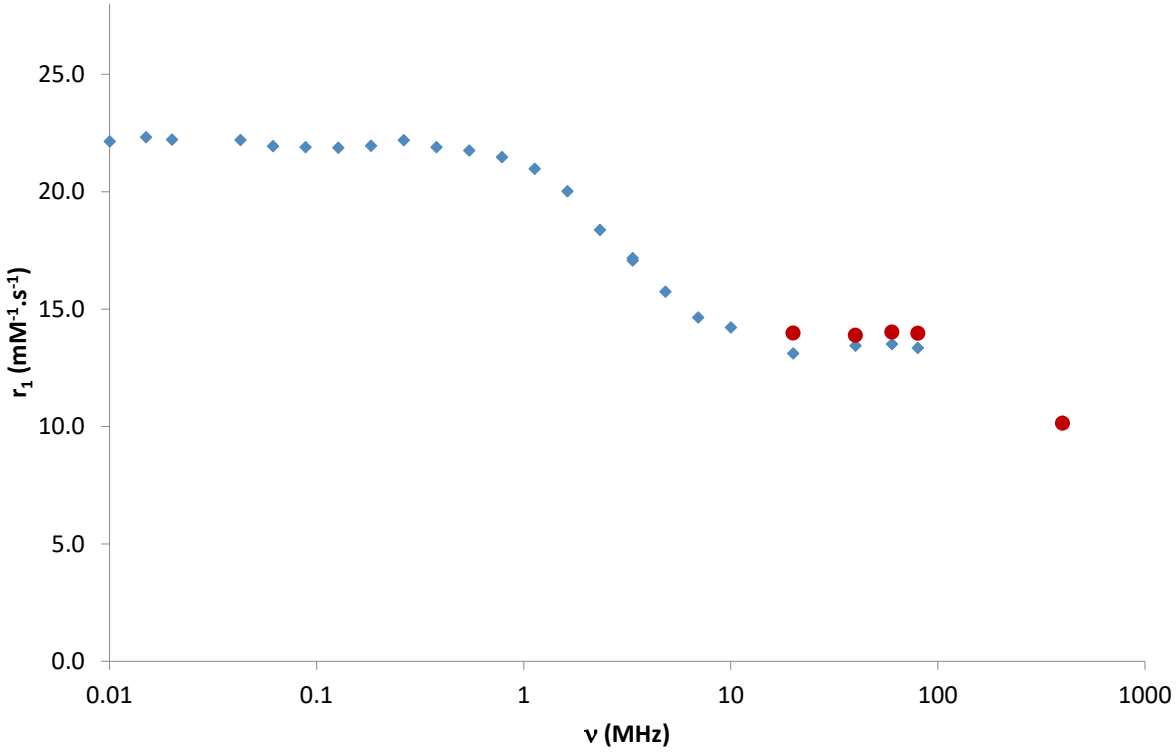

Figure S9: ^{1}H NMRD profiles of aqueous solutions in HEPES 0.1 M, pH = 7.4 at 298 K containing [**GdPyC4mDPA**] = 1.01 mM (♦), or [**GdPyC4mDPAZn**] = 0.95 mM (●).

Table S2: Best-fit-parameters obtained from the fitting of the ^{1}H NMRD profiles to the SBM theory

Parameters	GdPyC4mDPA	GdPy[c]
q^{a}	2	2
k_{ex}^{298} (10^{6} s^{-1})^{b}	9.3	9.3
$\Delta H^{\neq}$ (kJ mol^{-1})^{b}	50.4	50.4
E_R (kJ mol^{-1})	21 (2)	20.2

τ_R^{298} (ps)	185 (5)	92[d]
E_V (kJ mol^{-1})[b]	1	1
τ_V^{298} (ps)	9 (2)	2.8
Δ^2 (10^{19} s^{-2})	0.08 (1)	0.96
D_{GDH}^{298} (10^{-10} m^2 s^{-1})[a]	26	26
E_{DGH} (kJ mol^{-1})	10 (2)	11

[a] Fixed to 2 from the luminescence lifetime measurements obtained on the corresponding Eu^{3+} complexes[5] ; [b] Fixed during the fitting procedure; [c] From [6]; τ_{RO}

Table S3: Luminescence lifetimes of **EuPyC4mDPA** and determination of the corresponding hydration number in the presence of 0 and 1.0 eq of Zn^{2+}, and in the presence of HSA

	EuPyC4mDPA	**EuPyC4mDPAZn**	**EuPyC4mDPA-HSA**	**EuPyC4mDPAZn-HSA**
τ_{H2O} **(ms)**	0.39 (1)	0.38 (1)	0.40 (1)	0.43 (1)
τ_{D2O} **(ms)**	2.03 (1)	1.82 (1)	1.45 (1)	1.42 (1)
***q*[a]**	2.2 (3)	2.2 (3)	1.9 (3)	1.6 (3)

a. Calculated from ref [3]

$q = A\left(\tau_{H_2O}^{-1} - \tau_{D_2O}^{-1} - \alpha\right)$ with A=1.2 ms, α=0.25 ms^{-1}.

Table S4: Best-fit-parameters obtained from the fitting of the ^{1}H NMRD profiles to the SBM theory including the Lipari-Szabo approach

	GdPyC4mDPA	**GdPyC4mDPAZn**
q[a]	2	2
k_{ex}^{298} (10^6 s^{-1})[b]	9.3	9.3

$\Delta H^{\neq}$ (kJ.mol^{-1}) [b]	50	50
E_l (kJ.mol^{-1})	21 (2)	30 (6)
τ_l^{310} (ps)	78 (4)	65 (9)
E_g (kJ.mol^{-1})	11 (2)	15 (3)
τ_g^{310} (ps)	2300 (200)	2200 (200)
S^2	0.14 (1)	0.21 (1)
D_{GdH}^{298}(10^{-9} m^{2}s^{-1}) [c]	26	26
E_{DGdH} (kJ.mol^{-1})	31 (4)	44 (8)
τ_v^{310}(ps)	9.2 (4)	9.4 (5)
Δ^2(10^{20}s^{-1})	0.066 (1)	0.059 (1)

[a] Fixed to the values obtained from luminescence lifetime measurements from Table S5; [b] Fixed to the values of **GdPy**;[7] [c] Fixed during the fitting procedure;

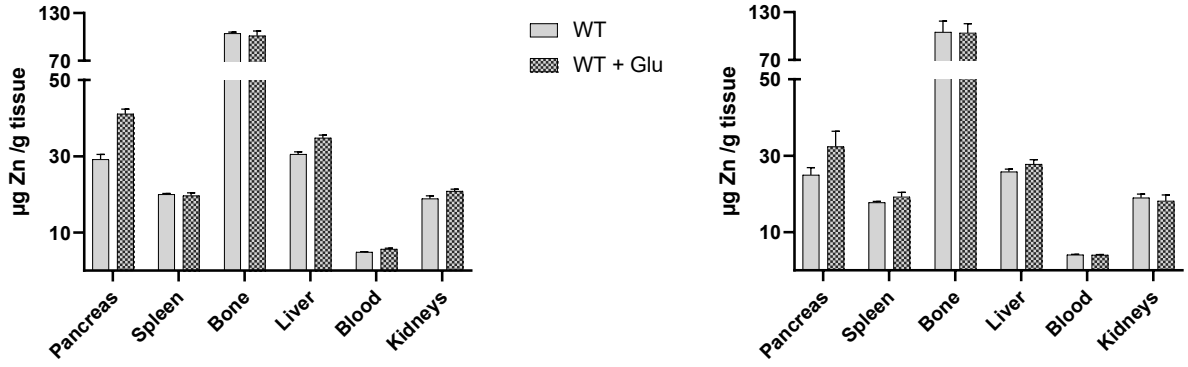

Figure S10: Zinc content in different tissues measured by ICP-OES for mice with glucose injection (WT + Glu) and control mice (WT). Animals were euthanized 20 min (left) or 1h10 (right) after glucose injection, and organs were excised and digested in HNO_3 prior to analysis; data are presented in µg of Zn per g of tissue (n = 6, ±SEM).

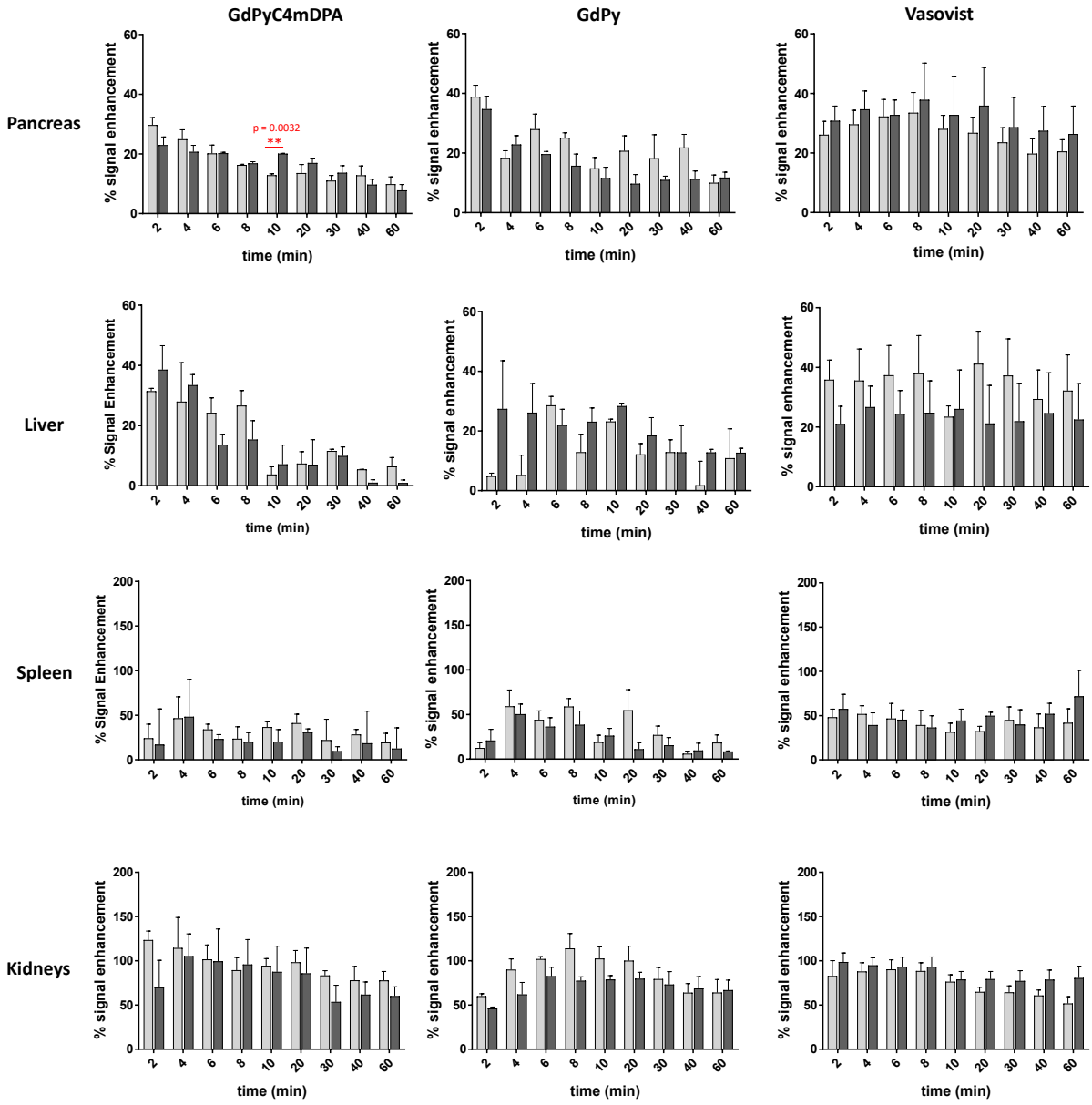

Figure S11: % of signal enhancement of the MRI images in different organs after intravenous contrast agent injection (**GdPyC4mDPA** or **GdPy** or **Vasovist®** 44 µmol.kg^{-1}) and with (dark grey) or without (light grey) glucose injection 10 min prior to contrast agent injection. The time in min corresponds to the time post iv injection of contrast agent. Data are presented as mean values (n = 3, ± SEM).

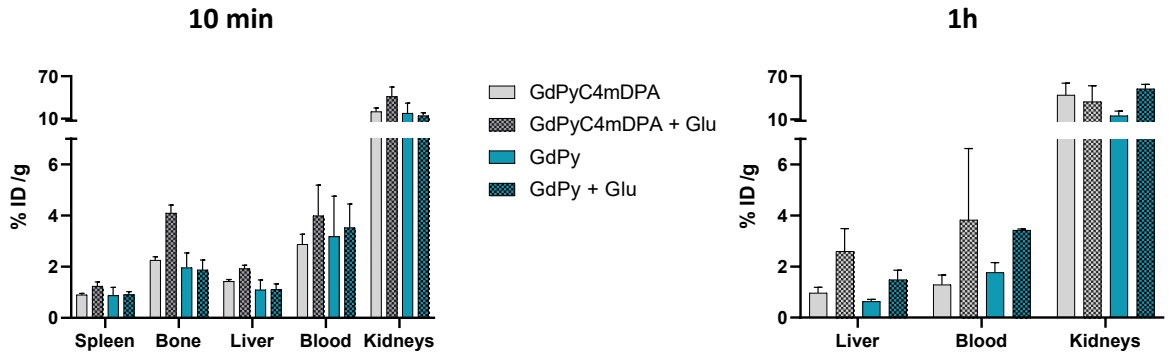

Figure S12: Gadolinium content in different organs measured by ICP-OES for mice with glucose injection (+ Glu) or control mice (WT). Animals were euthanized 10 min (left) or 1h (right) after contrast agent injection, and organs were excised and digested in HNO_3 prior to analysis; data are presented in % of injected dose per g of organ (n = 3, ±SEM). The Gd content 1h after contrast agent injection was too low to be detected in the bone and in the spleen.

Equations used for the fitting of NMRD data, with the SBM model including the model-free Lipari-Szabo approach

The measured longitudinal proton relaxation rate, R_1^{obs} = $1/T_1^{obs}$, is the sum of a paramagnetic and a diamagnetic contribution as expressed in Equation (A1), where r_1 is the proton relaxivity:

$$R_1^{obs} = R_1^d + R_1^p = R_1^d + r_1[\mathrm{Gd}^{3+}] \quad \text{(A1)}$$

The relaxivity can be divided into an inner and an outer sphere term as follows:

$$r_1 = r_{1is} + r_{1os} \quad \text{(A2)}$$

The inner sphere term is given in Equation (A3), where q is the number of inner sphere water molecules.[4]

$$r_{1is} = \frac{1}{1000} \times \frac{q}{55.55} \times \frac{1}{T_{1m}^{H} + \tau_m} \qquad \text{(A3)}$$

The longitudinal relaxation rate of inner sphere protons, $1/T_{1m}^{H}$ is expressed by Equation (A4), where r_{GdH} is the effective distance between the electron charge and the ^{1}H nucleus, ω_I is the proton resonance frequency and ω_S is the Larmor frequency of the Gd^{3+} electron spin.

$$\frac{1}{T_{1m}^{H}} = \frac{2}{15}\left(\frac{\mu_0}{4\pi}\right)^2 \frac{\hbar^2 \gamma_I^2 \gamma_S^2}{r_{GdH}^6} S(S+1) \times \left[3J(\omega_I;\tau_{d1}) + 7J(\omega_S;\tau_{d2})\right] \qquad \text{(A4)}$$

$$\frac{1}{\tau_{di}} = \frac{1}{\tau_m} + \frac{1}{\tau_{RH}} + \frac{1}{T_{ie}} \qquad \text{for } i = 1,2 \qquad \text{(A5)}$$

where τ_{RH} is the rotational correlation time of the Gd-H_{water} vector.

For small molecular weight chelates (fast rotation), the spectral density function is expressed as in Equation (A6).

$$J(\omega;\tau) = \left(\frac{\tau}{1 + \omega^2 \tau^2}\right) \qquad \text{(A6)}$$

For slowly rotating species, the spectral density functions are described the Lipari-Szabo approach.[8] In this model we distinguish two statistically independent motions; a rapid local motion with a correlation time τ_l and a slower global motion with a correlation time τ_g. Supposing the global molecular reorientation is isotropic, the relevant spectral density functions are expressed as in Equations (A7-A11), where the general order parameter S^2 describes the degree of spatial restriction of the local motion. If the local motion is isotropic, $S^2 = 0$; if the rotational dynamics is only governed by the global motion, $S^2 = 1$.

$$J(\omega_I;\tau_{d1})=\left(\frac{\mathcal{S}^2\tau_{d1g}}{1+\omega_I^2\tau_{d1g}^2}+\frac{(1-\mathcal{S}^2)\tau_{d1}}{1+\omega_I^2\tau_{d1}^2}\right) \tag{A7}$$

$$J(\omega_S;\tau_{d2})=\left(\frac{\mathcal{S}^2\tau_{d2g}}{1+\omega_S^2\tau_{d2g}^2}+\frac{(1-\mathcal{S}^2)\tau_{d2}}{1+\omega_S^2\tau_{d2}^2}\right) \tag{A8}$$

$$\frac{1}{\tau_{dig}}=\frac{1}{\tau_m}+\frac{1}{\tau_g}+\frac{1}{T_{ie}} \qquad i = 1, 2 \tag{A9}$$

$$\frac{1}{\tau}=\frac{1}{\tau_g}+\frac{1}{\tau_l} \tag{A10}$$

$$J_i(\omega_I)=\left(\frac{S^2\tau_g}{1+i^2\omega_I^2\tau_g^2}+\frac{(1-S^2)\tau}{1+i^2\omega_I^2\tau^2}\right) \qquad i = 1, 2 \tag{A11}$$

The rotational correlation time, τ_{RH} is assumed to have simple exponential temperature dependence with an E_R activation energy as given in Equation (A12).

$$\tau_{RH}=\tau_{RH}^{298}exp[\frac{E_R}{R}\left(\frac{1}{T}-\frac{1}{298.15}\right)] \tag{A12}$$

The outer-sphere contribution can be described by Equations (A13 and A14) where N_A is the Avogadro constant, and J_{os} is its associated spectral density function as given by Equation (A14).[8-9]

$$r_{1os}=\frac{32\,N_A\pi}{405}\left(\frac{\mu_0}{4\pi}\right)^2\frac{h^2\gamma_S^2\gamma_I^2}{a_{GdH}D_{GdH}}S(S+1)[3J_{os}(\omega_I,T_{1e})+7J_{os}(\omega_S,T_{2e})] \tag{A13}$$

$$J_{os}(\omega, T_{je}) = \mathrm{Re}\left[\frac{1+14\left(i\omega\tau_{GdH}+\frac{\tau_{GdH}}{T_{je}}\right)^{1/2}}{1+\left(i\omega\tau_{GdH}+\frac{\tau_{GdH}}{T_{je}}\right)^{1/2}+49\left(i\omega\tau_{GdH}+\frac{\tau_{GdH}}{T_{je}}\right)+19\left(i\omega\tau_{GdH}+\frac{\tau_{GdH}}{T_{je}}\right)^{3/2}}\right] \quad \text{(A14)}$$

$j = 1,2$

The longitudinal and transverse electronic relaxation rates, $1/T_{1e}$ and $1/T_{2e}$ are expressed by Equation (A15 and A16), where τ_v is the electronic correlation time for the modulation of the zero-field-splitting interaction, E_v the corresponding activation energy and Δ^2 is the mean square zero-field-splitting energy. We assumed a simple exponential dependence of τ_v versus $1/T$ as written in Equation (A17).

$$\left(\frac{1}{T_{1e}}\right)^{ZFS} = \frac{1}{25}\Delta^2\tau_v\{4S(S+1)-3\}\left(\frac{1}{1+\omega_S^2\tau_v^2}+\frac{4}{1+4\omega_S^2\tau_v^2}\right) \quad \text{(A15)}$$

$$\left(\frac{1}{T_{2e}}\right)^{ZFS} = \Delta^2\tau_v\left(\frac{5.26}{1+0.372\omega_S^2\tau_v^2}+\frac{7.18}{1+1.24\omega_S\tau_v}\right) \quad \text{(A16)}$$

$$\tau_v = \tau_v^{298}\exp\left[\frac{E_v}{R}\left(\frac{1}{T}-\frac{1}{298.15}\right)\right] \quad \text{(A17)}$$

The diffusion coefficient for the diffusion of a water proton away from a Gd^{3+} complex, D_{GdH}, is assumed to obey an exponential law versus the inverse of the temperature, with activation energy $E_{DGdH,}$ as given in Equation (A18). D_{GdH}^{298} is the diffusion coefficient at 298.15 K.

$$D_{GdH} = D_{GdH}^{298}\exp\left\{\frac{E_{GdH}}{R}\left(\frac{1}{298.15}-\frac{1}{T}\right)\right\} \quad \text{(A18)}$$

In the analysis of the data, several parameters have been fixed to common values. Among these, r_{GdO} has been fixed to 2.5, based on available crystal structures and electron nuclear double resonance (ENDOR) results,[8] and the quadrupolar coupling constant, $\chi(1+\eta^2/3)^{1/2}$, has been set to the value for pure water 7.58 MHz.[9] The Gd–water proton distance was fixed to r_{GdH}= 3.1, and the closest approach between the Gd^{3+} ion and the outer-sphere protons to

a_{GdH}= 3.6. The fitting has been restricted to NMRD data above 4 MHz as at low magnetic fields the SBM theory fails in describing electronic parameters and rotational dynamics of slowly rotating species.

[1] a) F. Yerly, in *OPTIMISEUR 2.3.5*, Lausanne, Switzerland, **1999**; b) F. Yerly, in *VISUALISEUR 2.3.5*, Lausanne, Switzerland, **1999**.

[2] R. M. Supkowski, W. D. Horrocks, *Inorg. Chem.* **1999**, *38*, 5616-5619.

[3] A. Beeby, I. M. Clarkson, R. S. Dickins, S. Faulkner, D. Parker, L. Royle, A. S. de Sousa, J. A. G. Williams, M. Woods, *J. Chem. Soc., Perkin Trans.* **1999**, 493-503.

[4] L. Sarka, L. Burai, E. Brucher, *Chem. Eur. J.* **2000**, *6*, 719-724.

[5] K. P. Malikidogo, I. Da Silva, J.-F. Morfin, S. Lacerda, L. Barantin, T. Sauvage, J. Sobilo, S. Lerondel, É. Tóth, C. S. Bonnet, *Chem. Commun.* **2018**, *54*, 7597-7600.

[6] C. S. Bonnet, F. Buron, F. Caille, C. M. Shade, B. Drahos, L. Pellegatti, J. Zhang, S. Villette, L. Helm, C. Pichon, F. Suzenet, S. Petoud, E. Toth, *Chem. Eur. J.* **2012**, *18*, 1419-1431.

[7] L. Pellegatti, J. Zhang, B. Drahos, S. Villette, F. Suzenet, G. Guillaumet, S. Petoud, E. Toth, *Chem. Commun.* **2008**, 6591-6593.

[8] Z. Luz, S. Meibomm, *J.Am.Chem.Soc.* **1964**, *86*, 4766-4768.

[9] F. A. Dunand, É. Tóth, R. Hollister, A. E. Merbach, *JBIC Journal of Biological Inorganic Chemistry* **2001**, *6*, 247-255.